

Properties of nuclear and Coulomb breakup of ${}^8\text{B}$

K. Ogata,^{1,*} T. Matsumoto,² Y. Iseri,³ and M. Yahiro¹

¹*Department of Physics, Kyushu University, Fukuoka 812-8581, Japan*

²*RIKEN Nishina Center, 351-0098 Wako, Japan*

³*Department of Physics, Chiba-Keizai College, Todoroki-cho 4-3-30, Inage, Chiba 263-0021, Japan*

(Dated: May 1, 2019)

Dependence of breakup cross sections of ${}^8\text{B}$ at 65 MeV/nucleon on target mass number A_T is investigated by means of the continuum-discretized coupled-channels method (CDCC) with more reliable distorting potentials than in preceding study. The scaling law of the nuclear breakup cross section as $A_T^{1/3}$ is found to be satisfied only in the middle A_T region of $40 \lesssim A_T \lesssim 150$. Interference between nuclear and Coulomb breakup amplitudes turns out to vanish at very forward angles with respect to the center-of-mass of ${}^8\text{B}$, independent of target nucleus. Truncation of the relative energy between the p and ${}^7\text{Be}$ fragments slightly reduces contribution from nuclear breakup at very forward angles, while the angular region in which the first-order perturbation theory works well does not change essentially.

PACS numbers: 24.10.Eq, 25.60.Gc, 25.70.De

Properties of unstable nuclei have been one of the most important subjects in nuclear physics. Breakup reactions of such short-lived nuclei provide us plentiful information on their static and dynamical features. Responses for electromagnetic transitions of unstable nuclei, which have been intensively studied in particular, are expected to be obtained by breakup reactions with a heavy target nucleus such as ${}^{208}\text{Pb}$ because of its dominant Coulomb field compared to the nuclear one. Recently, studies on two-neutron halo nuclei, e.g. ${}^6\text{He}$ and ${}^{11}\text{Li}$, based on this conjecture have been done and $B(E1)$ strengths and the spectroscopic factors were evaluated [1, 2]. Extraction of “pure” responses for electromagnetic transitions, however, requires accurate description of possible nuclear breakup, multistep transitions and the interference between nuclear and Coulomb breakup amplitudes. Systematic analysis [3] of breakup reactions of ${}^7\text{Be}$, ${}^8\text{B}$ and ${}^{11}\text{Be}$ with the continuum-discretized coupled-channels method (CDCC) [4] showed that the nuclear breakup cross section σ_N was scaled as $A_T^{1/3}$, where A_T is the target mass number. If the scaling is true, one can evaluate σ_N for heavy target such as ${}^{208}\text{Pb}$ from the measured breakup cross section for light target such as ${}^{12}\text{C}$ that is dominated by nuclear breakup. Hence, there is a possibility that one can remove the “contamination” due to nuclear breakup from the measured breakup cross section for heavy target that is in general due to both nuclear and Coulomb breakup. It was shown [3], however, also that one could not be free from the nuclear-Coulomb (N-C) interference, even if only the events corresponding to forward-angle scattering, in which the scattering angle of the center-of-mass (c.m.) of the projectile is small, are selected. Thus, accurate analysis of breakup reactions of unstable nuclei with CDCC will be necessary to draw a quantitative conclusion on $B(E1)$ values and spectro-

scopic factors. Four-body CDCC [5] analysis of breakup of ${}^6\text{He}$ and ${}^{11}\text{Li}$ are particularly interesting and important.

Before going to the four-body system, in this brief report we re-investigate the breakup reactions of ${}^8\text{B}$ nucleus at 65 MeV/nucleon by several target nuclei A , i.e., ${}^{12}\text{C}$, ${}^{16}\text{O}$, ${}^{40}\text{Ca}$, ${}^{58}\text{Ni}$, ${}^{90}\text{Zr}$, ${}^{152}\text{Sm}$ and ${}^{208}\text{Pb}$, with CDCC based on a ${}^7\text{Be}+p+A$ three-body model. The main purpose of the present study is to show the result based on more realistic p - A and ${}^7\text{Be}$ - A optical potentials. The $A_T^{1/3}$ scaling-law of σ_N and the N-C interference are investigated as in Ref. [3]. As an interesting point not analyzed in Ref. [3], we show the dependence of the N-C interference on the cut-off for the relative energy between the ${}^7\text{Be}$ and p fragments after breakup.

In the present CDCC calculation, we take the ${}^8\text{B}$ wave function of Ref. [6] for the p-wave, with neglecting the spin-orbit potential; the depth of the central part is determined to reproduce the proton separation energy $S_p = 137$ keV. For the s-wave the p - ${}^7\text{Be}$ potential of Barker [7] that reproduces the scattering length [8] for the channel spin $S = 2$ component is adopted. As for the d- and f-state potentials, we use the parameters of Ref. [9]. The intrinsic spins of p and ${}^7\text{Be}$ are neglected for simplicity. We take 20, 10, 10 and 5 discretized continuum states for the s-, p-, d- and f-waves, respectively. The maximum wave number (radius) between p and ${}^7\text{Be}$ is set to be 0.66 fm^{-1} (200 fm). When only nuclear breakup is included, the scattering waves between ${}^8\text{B}$ and the target are solved up to $R_{\text{max}} = 100$ fm. The values of R_{max} corresponding to the calculation with Coulomb breakup amplitudes are 210, 210, 250, 330, 450, 670 and 880 fm for ${}^{12}\text{C}$, ${}^{16}\text{O}$, ${}^{40}\text{Ca}$, ${}^{58}\text{Ni}$, ${}^{90}\text{Zr}$, ${}^{152}\text{Sm}$ and ${}^{208}\text{Pb}$ targets, respectively. The maximum orbital angular momentum L_{max} between ${}^8\text{B}$ and A is evaluated as $L_{\text{max}} = K R_{\text{max}}$, where K is the ${}^8\text{B}$ - A relative wave number in the incident channel. For the partial waves with $L > 1000$, the eikonal-CDCC method (E-CDCC) [10] is used to obtain S matrix elements.

*Electronic address: ogata@phys.kyushu-u.ac.jp

We adopt the global optical potential based on Dirac phenomenology (the EDAD1 parameter) [11] for the distorting potential between p and A . As for the ${}^7\text{Be}$ - A potential $U(R_7)$, we slightly modify the ${}^7\text{Li}$ global optical potential of Cook [12] that is appropriate around 10 MeV/nucleon as

$$U(R_7) = -74.03 \left\{ 1 + \exp \left[\frac{R_7 - 1.325A_T^{1/3}}{0.853} \right] \right\}^{-1} - iW(A_T) \left\{ 1 + \exp \left[\frac{R_7 - 1.640A_T^{1/3}}{0.809} \right] \right\}^{-1},$$

$$W(A_T) = 31.47 - 0.160A_T + 0.00045A_T^2.$$

Note that the diffuseness parameters are not changed and the A_T dependence appears only in the radial parameters and the depth of the imaginary part as in the original potential [12]. This potential is found to reproduce quite well the elastic cross sections of ${}^7\text{Li}$ - ${}^{12}\text{C}$ at 67.8 MeV/nucleon [13] and ${}^7\text{Be}$ - ${}^{208}\text{Pb}$ at 60.8 MeV/nucleon [14].

First we investigate the $A_T^{1/3}$ scaling law of σ_N , which is based on the following two assumptions [3]: 1) the partial breakup cross section $\sigma_N(L)$ is localized around L_0 , which is to be assumed as the glazing orbital angular momentum $L_g \equiv K(R_P + R_T)$, where R_P (R_T) is the radius of the projectile (target), and 2) the transmission coefficient T_L at L_0 is independent of the target nucleus. In Fig. 1 we show the $\sigma_N(L)$ calculated with CDCC,

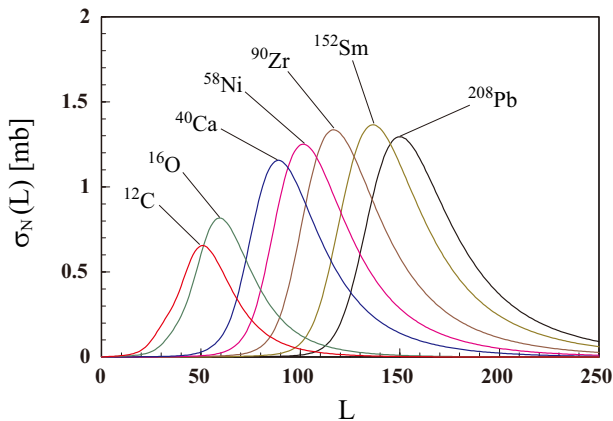


FIG. 1: (Color online) The partial cross sections for nuclear breakup of ${}^8\text{B}$ by the seven target nuclei concerned.

neglecting Coulomb breakup, for the seven target nuclei; the values of L_0/K and $T_{L_0} \equiv \sigma_N(L_0)K^2/[\pi(2L_0 + 1)]$ extracted are shown in Table I. One can find that L_0/K is scaled very well as $A_T^{1/3}$, i.e., $L_0/K \approx 1.4A_T^{1/3} + 2.7$, which justifies the interpretation of the L_0/K extracted as $R_P + R_T$. The corresponding T_{L_0} shows, however, clear target dependence; in the middle A_T region of $40 \leq A_T \leq 152$, T_{L_0} is almost constant, while T_{L_0} significantly decreases for $A_T \leq 16$ and $A_T = 208$. This indicates that

TABLE I: L_0/K and T_{L_0} extracted from the partial cross sections shown in Fig. 1. See the text for details.

A	${}^{12}\text{C}$	${}^{16}\text{O}$	${}^{40}\text{Ca}$	${}^{58}\text{Ni}$	${}^{90}\text{Zr}$	${}^{152}\text{Sm}$	${}^{208}\text{Pb}$
L_0/K [fm]	6.02	6.27	7.54	8.15	9.00	10.1	11.0
T_{L_0}	0.14	0.19	0.29	0.30	0.31	0.28	0.25

the nuclear absorption at $R_P + R_T$ due to the imaginary parts of the p - A and ${}^7\text{Be}$ - A optical potentials is strong compared to the coupling potentials that causes breakup, in the reactions with very light or very heavy target.

Therefore, the $A_T^{1/3}$ scaling law of σ_N is considered to hold in $40 \lesssim A_T \lesssim 152$ region, as shown in Fig. 2; the proportional constant is found to be 12.8. Note that

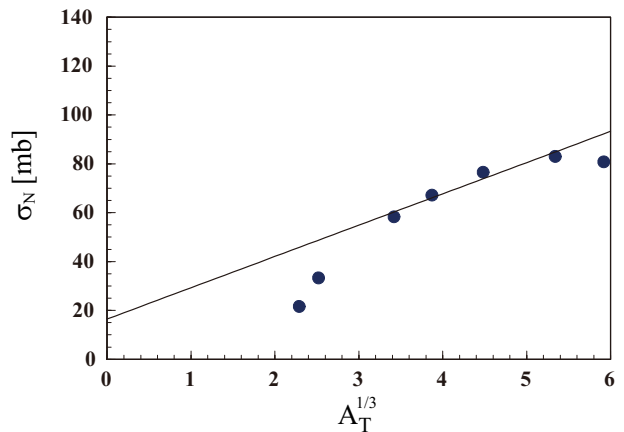


FIG. 2: The nuclear breakup cross section σ_N plotted with respect to $A_T^{1/3}$. The solid line shows the scaled result: $\sigma_N = 12.8A_T^{1/3} + 16.5$ obtained by fitting of the σ_N for ${}^{40}\text{Ca}$, ${}^{58}\text{Ni}$, ${}^{90}\text{Zr}$ and ${}^{208}\text{Pb}$ targets.

whether the $A_T^{1/3}$ scaling law is satisfied is determined by the properties of the distorting potentials used in CDCC calculation, which dictates the actual A_T dependence of T_{L_0} . In order to perform systematic analysis of breakup reactions of ${}^{11}\text{Be}$, ${}^7\text{Be}$, ${}^6\text{He}$, ${}^{11}\text{Li}$ etc. with three-body or four-body CDCC, therefore, reliable optical potentials between the fragments of the projectile and the targets are necessary.

Next we show in Fig.3 the deviation (relative difference) of the breakup cross section σ_C^{pert} calculated with first-order perturbative CDCC from the cross section $\sigma_{NC}^{\text{full}}$ calculated with full CDCC; in the former calculation the one-step process due to monopole and dipole transitions are included but nuclear breakup processes and multistep ones are neglected, and in the latter all processes due to nuclear and Coulomb breakup are included. These cross sections are integrated over the relative energy ϵ between the p and ${}^7\text{Be}$ fragments up to 10 MeV. The solid, dashed, dotted and dash-dotted lines indicate the results corresponding to ${}^{12}\text{C}$, ${}^{40}\text{Ca}$, ${}^{90}\text{Zr}$ and ${}^{208}\text{Pb}$ targets, respectively. The horizontal axis is the

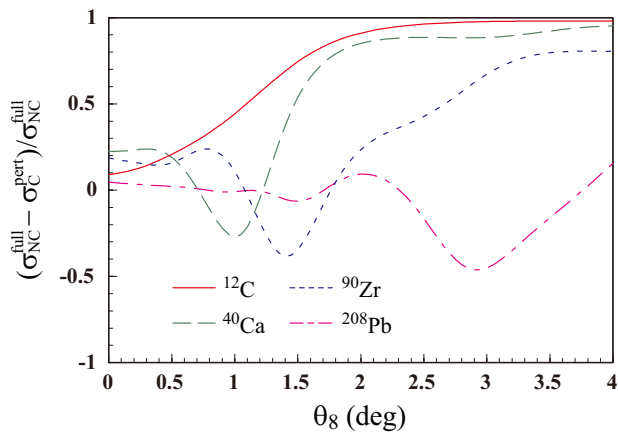


FIG. 3: (Color online) Relative difference between the breakup cross sections calculated with full CDCC and first-order perturbative CDCC, as a function of θ_8 . The solid, dashed, dotted and dash-dotted lines correspond to the breakup with ^{12}C , ^{40}Ca , ^{90}Zr and ^{208}Pb targets, respectively.

c.m. scattering angle θ_8 of ^8B . As expected, the difference is very large except at forward angles because of dominant contribution from nuclear breakup. It should be noted, however, that even at very forward angles $\theta_8 \sim 0^\circ$ the difference is somewhat large, i.e., about 10–20 %, for the breakup with ^{12}C , ^{58}Ni and ^{90}Zr targets. On the other hand, for the breakup with ^{208}Pb target, the difference is less than 10% for $\theta_8 \leq 2.4^\circ$, which justifies in part the use of the first-order perturbation theory to extract “pure” responses of ^8B to electromagnetic transitions in analysis of ^8B breakup by ^{208}Pb . The possible 10% error of such simplified analysis, however, should be kept in mind.

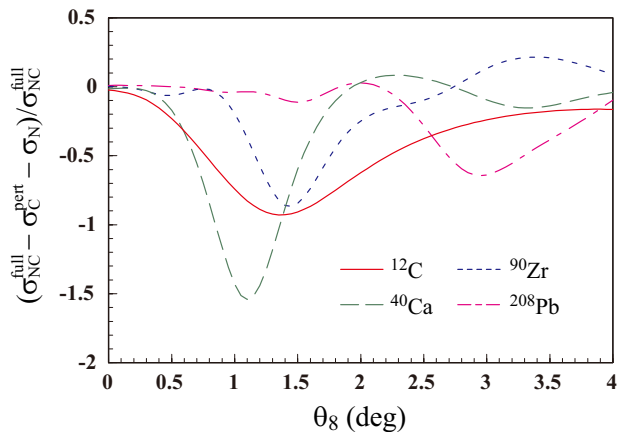


FIG. 4: (Color online) Same as in Fig. 3 but for the relative difference between the breakup cross section with full CDCC and that with first-order perturbative CDCC added by the nuclear breakup cross section.

Figure 4 shows the relative difference between $\sigma_{NC}^{\text{full}}$ and $\sigma_C^{\text{pert}} + \sigma_N$. This quantity shows the importance

of the N-C interference, since it vanishes when there is no N-C interference; note that multistep processes due to Coulomb breakup are negligible. Except for the ^{208}Pb target case, the interference is crucially important for $1.0^\circ \lesssim \theta_8 \lesssim 2.0^\circ$. This difference is closely related to the value shown in Fig. 3 of Ref. [3], in which it was concluded that the contribution from the interference tended to vanish only for ^8B projection on ^{208}Pb target. Our present calculation shows, however, that the contribution from the interference almost vanishes at $\theta_8 \sim 0^\circ$ for all target nuclei. Table II shows the maximum scattering angle θ_{cr} of the region in which the contribution from the N-C interference is less than 10%, together with the corresponding impact parameters b_{cr} , for the seven reactions concerned. It is found by detailed analysis that

TABLE II: The values of θ_{cr} and b_{cr} . See the text for details.

A	^{12}C	^{16}O	^{40}Ca	^{58}Ni	^{90}Zr	^{152}Sm	^{208}Pb
θ_{cr} [deg]	0.30	0.30	0.40	0.60	0.90	1.65	2.30
b_{cr} [fm]	26.5	31.8	47.6	42.1	38.4	31.4	29.4

for nuclear breakup, transition of ^8B to the p-wave continuum is dominant at very forward angles, since the monopole coupling potentials are significantly larger than those with other multipolarities and multistep excitations are negligibly small in that region. On the other hand, for Coulomb breakup, dipole transition is dominant at forward angles and consequently s- and d-wave breakup cross sections are dominant. Thus, the final states of ^8B corresponding to the nuclear and Coulomb breakup are different from each other with respect to the orbital angular momentum between ^7Be and p . This is the reason for the vanishment of the N-C interference at $\theta_8 \sim 0^\circ$. Note that the dominance of the monopole coupling potentials due to nuclear breakup actually depends on the p - A and ^7Be - A potentials. Accurate evaluation of the distorting potentials in CDCC calculation is, again, of crucial importance.

It is sometime conjectured that contribution from nuclear breakup can be quenched if ϵ is truncated at a certain small value ϵ_0 . We show in Fig. 5 the relative difference between the breakup cross sections calculated with full CDCC and first-order perturbative CDCC as in Fig. 3 but with the truncation at $\epsilon_0 = 0.5$ MeV (the solid lines), 1 MeV (the dashed lines) and 2 MeV (the dotted lines), together with the results with no truncation (the dash-dotted lines). The thick (thin) lines show the results with ^{12}C (^{208}Pb) target. One sees that the truncation of the excitation energy slightly reduces the relative difference at $\theta_8 \sim 0^\circ$. For $\theta_8 \gtrsim 0.5^\circ$ (2°) for the ^{12}C (^{208}Pb) target case, however, the difference is still very large, which indicates that even if truncation of ϵ is made, the first-order perturbation calculation will bring about serious error in analysis of the breakup reactions in this angular region, hence in values of the extracted $B(E1)$ and the spectroscopic factor. It should be remarked that in the breakup reaction with ^{208}Pb target θ_{cr} is shifted to the forward direction when the truncation is made.

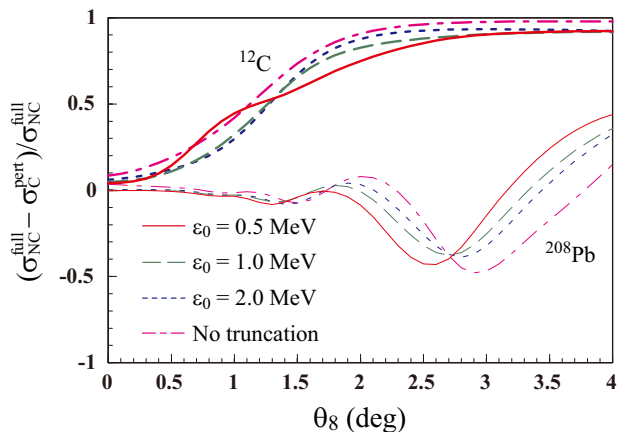


FIG. 5: (Color online) Relative error of the breakup cross section calculated with first-order perturbative CDCC from that with full CDCC. The solid, dashed and dotted lines correspond to the results with truncation of ϵ at 0.5 MeV, 1.0 MeV and 2.0 MeV, respectively. The results with no truncation are also shown by the dash-dotted lines. The thick (thin) lines correspond to the breakup with ^{12}C (^{208}Pb) target.

In summary, we re-investigate the nuclear and Coulomb breakup properties of ^8B at 65 MeV/nucleon by means of the continuum-discretized coupled-channels method (CDCC) with possibly more reliable p -target and ^7Be -target optical potentials than in the foregoing work [3]. The scaling law of the nuclear breakup cross section σ_N as $A_T^{1/3}$, where A_T is the target mass number, is found to be satisfied only in the middle mass region, i.e., $40 \lesssim A_T \lesssim 152$. The interference between nuclear

and Coulomb breakup amplitudes, the N-C interference, is very important even at forward angles $1^\circ \lesssim \theta_8 \lesssim 2^\circ$, where θ_8 is the scattering angle of the center-of-mass of ^8B . For the breakup with ^{208}Pb target, it is found that both contribution from σ_N and the N-C interference are not so important, i.e., less than 10%, for $\theta_8 \lesssim 2.4^\circ$. The present calculation shows that the N-C interference indeed tends to vanish at $\theta_8 \sim 0^\circ$, independent of target nucleus, in contrast to the conclusion of Ref. [3]. Also clarified is that the truncation of the relative energy between the p and ^7Be fragments on the measured breakup cross sections quenches the error of the first-order perturbation theory at $\theta_8 \sim 0^\circ$ but not helpful at all for $\theta_8 \gtrsim 0.5^\circ$ (2.0°) in the breakup with ^{12}C (^{208}Pb) target. One may conclude from the present study that the $B(E1)$ strength of ^8B can be extracted with quite small error of about 10% from analysis of the breakup cross section with ^{208}Pb for $\theta_8 \lesssim 2.4^\circ$ by means of the first-order perturbation theory. Nevertheless, assessment of the error of the perturbation theory with CDCC is extremely important because it does depend on the reaction system and incident energy. Our final remark is that all the results obtained in the present work reflect properties of the optical potentials used in the CDCC calculation. For systematic analysis of breakup reactions of ^{11}Be , ^7Be , ^6He , ^{11}Li etc. with CDCC, accurate evaluation of the optical potentials concerned is necessary.

KO acknowledges S. Bishop for providing elastic cross section data for ^7Be - ^{208}Pb scattering at 60.8 MeV/nucleon. The computation was mainly carried out using the computer facilities at Research Institute for Information Technology, Kyushu University.

-
- [1] T. Aumann *et al.*, Phys. Rev. C **59**, 1252 (1999); J. Wang *et al.*, Phys. Rev. C **65**, 034306 (2002).
 - [2] T. Nakamura *et al.*, Phys. Rev. Lett. **96**, 252502 (2006) and the references cited therein.
 - [3] M. S. Hussein, R. Lichtenthaler, F. M. Nunes and I. J. Thompson, Phys. Lett. **B640**, 91 (2006).
 - [4] M. Kamimura *et al.*, Prog. Theor. Phys. Suppl. **89**, 1 (1986); N. Austern *et al.*, Phys. Rep. **154**, 125 (1987).
 - [5] T. Matsumoto *et al.*, Phys. Rev. C **70**, 061601(R) (2004); T. Matsumoto *et al.*, Phys. Rev. C **73**, 051602(R) (2006).
 - [6] H. Esbensen and G. F. Bertsch, Nucl. Phys. **A600**, 66 (1996).
 - [7] F. C. Barker, Aust. J. Phys. **33**, 177 (1980).
 - [8] C. Angulo *et al.*, Nucl. Phys. **A716**, 211 (2003).
 - [9] S. Typel, H. H. Wolter, and G. Baur, Nucl. Phys. **A613**, 147 (1997).
 - [10] K. Ogata, M. Yahiro, Y. Iseri, T. Matsumoto and M. Kamimura, Phys. Rev. C **68**, 064609 (2003); K. Ogata, S. Hashimoto, Y. Iseri, M. Kamimura and M. Yahiro, Phys. Rev. C **73**, 024605 (2006).
 - [11] S. Hama, B. C. Clark, E. D. Cooper, H. S. Sherif, and R. L. Mercer, Phys. Rev. C **41** 2737 (1990); E. D. Cooper, S. Hama, B. C. Clark, and R. L. Mercer, Phys. Rev. C **47**, 297 (1993).
 - [12] J. Cook, Nucl. Phys. **A388**, 153 (1982).
 - [13] M. D. Cortina-Gil *et al.*, Phys. Lett. **B401**, 9 (1997).
 - [14] S. Bishop, private communication.